Synthesis, Structures, and Olefin Polymerization Characteristics of Group 4 Catalysts [Zr{(OAr)$_2$py}Cl$_2$(D)] (D = O-Donors, Cl[HPR$_3$]) Supported by Tridentate Pyridine-2,6-bis(aryloxide) Ligands

Michael C. W. Chan,*[,§] Ka-Ho Tam,[†] Nianyong Zhu,[†] Pauline Chiu,[†] and Shigekazu Matsui[‡]

Department of Biology and Chemistry, City University of Hong Kong, Tat Chee Avenue, Kowloon, Hong Kong, China, Department of Chemistry and HKU-CAS Joint Laboratory for New Materials, The University of Hong Kong, Pokfulam Road, Hong Kong, China, and R&D Center, Mitsui Chemicals, Inc., 580-32 Nagaura, Sodegaura, Chiba 299-0265, Japan.

Received October 6, 2005

The Zr(IV) complexes [Zr(L^1)X$_2$(D)] [H$_2$L^1 = 2,6-di(3-*tert*-butyl-5-methylphen-2-ol)pyridine; X = Cl, D = thf (**1**), OEt$_2$ (**2**), acetophenone (**3**), benzophenone (**4**), 2-acetonaphthone (**5**), Cl[HPR$_3$] {R = Me (**6**), Et (**7**); R$_3$ = Me$_2$Ph (**8**)}; X = CH$_2$Ph (**9**)] have been synthesized, and the crystal structures of **3**, **4**, and **7** have been determined. These catalysts, assisted by the robustness and chelating strength of the pyridine-bis(phenolate) moiety, exhibit excellent activities for ethylene polymerization in conjunction with MAO. Studies to assess the impact of the donor group during the catalytic process suggest that the same active species is generated by **1**−**8**/MAO and the donor group does not play an active role. Even higher activities are observed for the **1**/^{i}Bu$_3$Al/Ph$_3$CB(C$_6$F$_5$)$_4$ system in ethylene polymerization and propylene copolymerization reactions (36 590 and 15 700 g of polymer (mmol of catalyst)$^{-1}$ h^{-1}, respectively), with the latter displaying good C3 incorporation (25.4 mol % C3). Insight into the catalytic behavior of the **1**/MAO system has been derived from GPC and NMR characterization of the polymers prepared under different reaction conditions. ^{1}H and ^{13}C NMR end-group analyses reveal resonances for saturated methyl chain-end groups only and undetectable or negligible levels of unsaturated vinyl chain ends. This indicates that for the polymerization chain-transfer mechanism, the conventional β-H transfer reactions to the metal/monomer are insignificant and the unusual chain transfer to Al pathway is vastly dominant.

Introduction

Aryloxide- and alkoxide-based chelating ligands have proved to be a success story in the advancement of post-metallocene polyolefin catalysts.[1] The underlying design strategy has targeted non-cyclopentadienyl species that are isoelectronic with the [Cp$_2$Zr] moiety, and the employment of multidentate alkoxide auxiliaries has expanded the range of environments around the catalytic active site. Bidentate ligand sets of the type [O,O] and [O,L]$_2$ have been particularly prominent.[2] Notably, Fujita and co-workers have pioneered a family of bis(phenoxyimine) group 4 polyolefin catalysts that are remarkable for their ultrahigh activities and versatile polymerization capabilities.[3] The ability of tetradentate [O$_2$L$_2$] (L = imine, amine, sulfide) ligands to mediate octahedral catalytic centers has also been extensively explored.[4] Linearly linked [O$_2$L$_2$] auxiliaries typically coordinate to the metal in a "α-*cis*" configuration to afford C_2-symmetric structures, and this has been instrumental in the development

* To whom correspondence should be addressed. E-mail: mcwchan@cityu.edu.hk. Fax: +852 2788 7406.

§ City University of Hong Kong.

† The University of Hong Kong.

‡ Mitsui Chemicals, Inc.

(1) Reviews: (a) Gibson, V. C.; Spitzmesser, S. K. *Chem. Rev.* **2003**, *103*, 283. (b) Suzuki, Y.; Terao, H.; Fujita, T. *Bull. Chem. Soc. Jpn*. **2003**, *76*, 1493. (c) Kawaguchi, H.; Matsuo, T. *J. Organomet. Chem*. **2004**, *689*, 4228.

(2) (a) van der Linden, A.; Schaverien, C. J.; Meijboom, N.; Ganter, C.; Orpen, A. G. *J. Am. Chem. Soc.* **1995**, *117*, 3008. (b) Matilainen, L.; Klinga, M.; Leskelä, M. *J. Chem. Soc., Dalton Trans*. **1996**, 219. (c) Bei, X.; Swenson, D. C.; Jordan, R. F. *Organometallics* **1997**, *16*, 3282. (d) Tsukahara, T.; Swenson, D. C.; Jordan, R. F. *Organometallics* **1997**, *16*, 3303. (e) Kim, I.; Nishihara, Y.; Jordan, R. F.; Rogers, R. D.; Rheingold, A. L.; Yap, G. P. A. *Organometallics* **1997**, *16*, 3314. (f) Fokken, S.; Spaniol, T. P.; Okuda, J.; Sernetz, F. G.; Mülhaupt, R. *Organometallics* **1997**, *16*, 4240. (g) Hustad, P. D.; Tian, J.; Coates, G. W. *J. Am. Chem. Soc.* **2002**, *124*, 3614. (h) Oakes, D. C. H.; Kimberley, B. S.; Gibson, V. C.; Jones, D. J.; White, A. J. P.; Williams, D. J. *Chem. Commun*. **2004**, 2174. (i) Jones, D. J.; Gibson, V. C.; Green, S. M.; Maddox, P. J.; White, A. J. P.; Williams, D. J. *J. Am. Chem. Soc.* **2005**, *127*, 11037.

(3) (a) Matsui, S.; Mitani, M.; Saito, J.; Tohi, Y.; Makio, H.; Matsukawa, N.; Takagi, Y.; Tsuru, K.; Nitabaru, M.; Nakano, T.; Tanaka, H.; Kashiwa, N.; Fujita, T. *J. Am. Chem. Soc.* **2001**, *123*, 6847. (b) Mitani, M.; Mohri, J.; Yoshida, Y.; Saito, J.; Ishii, S.; Tsuru, K.; Matsui, S.; Furuyama, R.; Nakano, T.; Tanaka, H.; Kojoh, S.; Matsugi, T.; Kashiwa, N.; Fujita, T. *J. Am. Chem. Soc*. **2002**, *124*, 3327. (c) Mitani, M.; Furuyama, R.;. Mohri, J.; Saito, J.; Ishii, S.; Terao, H.; Nakano, T.; Tanaka, H.; Fujita, T. *J. Am. Chem. Soc*. **2003**, *125*, 4293. (d) Mitani, M.; Nakano, T.; Fujita, T. *Chem. Eur. J*. **2003**, *9*, 2396. (e) Mitani, M.; Saito, J.; Ishii, S.; Nakayama, Y.; Makio, H.; Matsukawa, N.; Matsui, S.; Mohri, J.; Furuyama, R.;. Terao, H.; Bando, H.; Tanaka, H.; Fujita, T. *Chem. Rec*. **2004**, *4*, 137. (f) Makio, H.; Fujita, T. *Bull. Chem. Soc. Jpn*. **2005**, *78*, 52.

(4) (a) Tjaden, E. B.; Swenson, D. C.; Jordan, R. F.; Petersen, J. L. *Organometallics* **1995**, *14*, 371. (b) Repo, T.; Klinga, M.; Pietikäinen, P.; Leskelä, M. Uusitalo, A.-M.; Pakkanen, T.; Hakala, K.; Aaltonen, P.; Löfgren, B. *Macromolecules* **1997**, *30*, 171. (c) Woodman, P. R.; Munslow, I. J.; Hitchcock, P. B.; Scott, P. *J. Chem. Soc., Dalton Trans*. **1999**, 4069. (d) Corden, J. P.; Errington, W.; Moore, P.; Wallbridge, M. G. H. *Chem. Commun*. **1999**, 323. (e) Toupance, T.; Dubberley, S. R.; Rees, N. H.; Tyrrell, B. R. Mountford, P. *Organometallics* **2002**, *21*, 1367. (f) Lavanant, L.; Chou, T.-Y.; Chi, Y.; Lehmann, C. W.; Toupet, L.; Carpentier, J. F. *Organometallics* **2004**, *23*, 5450. (g) Cuomo, C.; Strianese, M.; Cuenca, T.; Sanz, M.; Grassi, A. *Macromolecules* **2004**, *37*, 7469. (h) Yao, Y.; Ma, M.; Xu, X.; Zhang, Y.; Shen, Q.; Wong, W.-T. *Organometallics* **2005**, *24*, 4014.

10.1021/om050864z CCC: $33.50
Publication on Web 01/06/2006

of catalysts for the isospecific polymerization of 1-hexene[5] and styrene,[6] the former in a living fashion.

The focus on polyolefin catalysts supported by tridentate alkoxide ligands has been less intense. Pioneered by Kakugo[7] using the thio-bis(phenoxide) group, dianionic [O,L,O] ligands can adopt *fac* or *mer* geometry depending on the bite angle and flexibility of the backbone,[8] and interesting copolymerization studies have been reported.[9] However, many of the resultant catalysts are characterized by modest activities and fragile, noninert ligand frameworks, and this is especially true for donor-bis(alkoxide) derivatives.[10] Hence the factors affecting catalyst performance and polymerization behavior for tridentate systems have yet to be elucidated. Kol and Goldschmidt have recently described a class of bis(benzyl) group 4 complexes with tetradentate ligands derived from amine-bis(aryloxide) plus a sidearm O-, N-, or S-donor, which display excellent activities in the polymerization of 1-hexene.[11] The significance of the pendant arm has been emphasized because it is proposed to play a crucial role in determining the rates of the propagation and termination processes, thought to remain attached to the catalytic site, and is instrumental in achieving high activities. Indeed, the analogous tridentate amine-bis(aryloxide) catalysts without a sidearm donor have been observed to deactivate rapidly and give only traces of oligomers.

We became attracted to the application of tridentate pyridine-2,6-bis(aryloxide) groups as supporting ligands for polyolefin catalysts. We envisaged that the pyridine-bis(aryloxide) unit would provide a rigid and stable platform with chemically robust and strongly chelating functionalities. Our preliminary report[12] on the solvent-bound catalyst $[Zr\{(OAr)_2py\}Cl_2(thf)]$ described impressive activities for ethylene polymerization despite similarities with Kol's tridentate congeners. We now present a detailed account of the preparation, characterization, and olefin polymerization behavior of a series of Zr(IV) complexes $[Zr\{(OAr)_2py\}Cl_2(D)]$, where D represents a variety of O-donors (ethers, ketones) and $Cl[HPR_3]$ moieties. Complexes bearing different D groups are readily accessible and several crystal structures have been determined, while the impact of the donor upon the catalytic center and polymerization process has been probed. Significantly, excellent activities are observed for ethylene polymerization and copolymerization reactions, and the polymer characterization data indicate that the polymerization chain-transfer pathway is dominated by chain transfer to Al.

Scheme 1

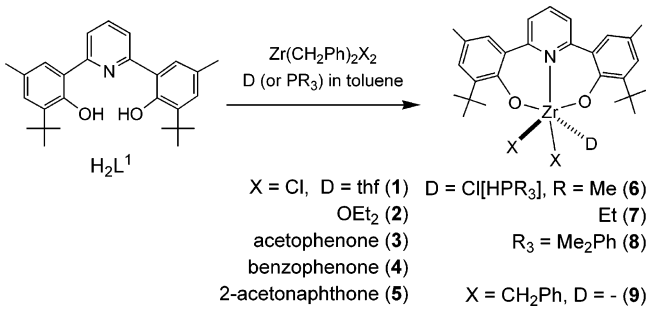

Results and Discussion

Synthesis and Characterization. The symmetric *tert*-butyl-bearing pyridine-2,6-bis(phenol) H_2L^1 was obtained in multigram quantities by the $Ni(dppe)Cl_2$-catalyzed coupling reaction of the Grignard reagent derived from the substituted 2-bromoanisole with 2,6-dibromopyridine,[13] followed by demethylation with molten pyridine hydrochloride at 210 °C.[14] On the basis of established procedures for related group 4 complexes,[2d,10a] we attempted to synthesize the $[Zr(L^1)Cl_2]$ target by the slow addition of Li_2L^1 to $ZrCl_4$ in toluene and THF or Et_2O at −78 °C. This yielded the solvated complexes $[Zr(L^1)Cl_2(D)]$ [D = thf (**1**), OEt_2 (**2**)] in moderate yields (ca. 60%). However, considerable care must be taken for this procedure in order to avert the facile formation of the bis-ligand species $[Zr(L^1)_2]$, which becomes the major product if the rate of addition for Li_2L^1 is excessive, if ketone/phosphine donors are used, or in the absence of a strongly donating solvent/ligand. A more convenient preparative route to complexes **1**−**5** involves the treatment of $Zr(CH_2Ph)_2Cl_2$ with H_2L^1 in toluene in the presence of excess donor (Scheme 1). The importance of the donor group is underscored by the observation that in their absence, intractable yellow precipitates are produced. Rather than Zr-coordinated PR_3 species, the use of phosphine donors in this reaction afforded **6**−**8**, which contain three chloride ligands bound to the anionic zirconium fragments and protonated phosphine moieties, as demonstrated by the X-ray structural determination of **7** (see below).

The bis(benzyl) Zr(IV) derivative of L^1 can also be synthesized, but a judicious choice of reaction solvent is required. Slow addition of H_2L^1 to $Zr(CH_2Ph)_4$ in Et_2O or pentane at −78 °C resulted in the precipitation of the five-coordinate $Zr(L^1)(CH_2Ph)_2$ (**9**) as a pale yellow solid. In contrast, employment of a solvent in which **9** readily dissolves (e.g., toluene, THF) yielded significant amounts of the octahedral product $[Zr(L^1)_2]$. All complexes have been fully characterized by ^1H, ^{13}C, and ^{31}P (for **6**−**8**) NMR spectroscopy. The broad ^1H NMR resonances for the ether and ketone donor groups are attribute to their displacement/recoordination or restricted rotation. The protonation of the phosphine atom in **6**−**8** is evident in their ^1H

(5) Tshuva, E. Y.; Goldberg, I.; Kol, M. *J. Am. Chem. Soc.* **2000**, *122*, 10706.

(6) (a) Capacchione, C.; Proto, A.; Eberling, H.; Mülhaupt, R.; Möller, K.; Spaniol, T. P.; Okuda, J. *J. Am. Chem. Soc.* **2003**, *125*, 4964. (b) Capacchione, C.; Manivannan, R.; Barone, M.; Beckerle, K.; Centore, R.; Oliva, L.; Proto, A.; Tuzi, A.; Spaniol, T. P.; Okuda, J. *Organometallics* **2005**, *24*, 2971.

(7) Miyatake, T.; Mizunuma, K.; Seki, Y.; Kakugo, M. *Makromol. Chem., Rapid Commun.* **1989**, *32*, 1131.

(8) (a) Fokken, S.; Spaniol, T. P.; Kang, H.-C.; Massa, W.; Okuda, J. *Organometallics* **1996**, *15*, 5069. (b) Nakayama, Y.; Watanabe, K.; Ueyama, N.; Nakamura, A.; Harada A.; Okuda, J. *Organometallics* **2000**, *19*, 2498. (c) Aihara, H.; Matsuo, T.; Kawaguchi, H. *Chem. Commun.* **2003**, 2204. (d) Trianionic [O,O,O] analogue: Matsuo, T.; Kawaguchi, H.; Sakai, M. *J. Chem. Soc., Dalton Trans.* **2002**, 2536. (e) Cyclometalated [O,N,C] analogue: Kui, S. C. F.; Zhu, N.; Chan, M. C. W. *Angew. Chem., Int. Ed.* **2003**, *42*, 1628.

(9) (a) Miyatake, T.; Mizunuma, K.; Kakugo, M. *Makromol. Chem., Macromol. Symp.* **1993**, *66*, 203. (b) Sernetz, F. G.; Mülhaupt, R.; Fokken, S.; Okuda, J. *Macromolecules* **1997**, *30*, 1562.

(10) (a) Mack, H.; Eisen, M. S. *J. Chem. Soc., Dalton Trans.* **1998**, 917. (b) Shao, P.; Gendron, R. A. L.; Berg, D. J.; Bushnell, G. W. *Organometallics* **2000**, *19*, 509. (c) Gauvin, R. M.; Osborn, J. A.; Kress, J. *Organometallics* **2000**, *19*, 2944. (d) Manivannan, R.; Sundararajan, G. *Macromolecules* **2002**, *35*, 7883.

(11) (a) Tshuva, E. Y.; Goldberg, I.; Kol, M.; Weitman, H.; Goldschmidt, Z. *Chem. Commun.* **2000**, 379. (b) Tshuva, E. Y.; Goldberg, I.; Kol, M.; Goldschmidt, Z. *Organometallics* **2001**, *20*, 3017. (c) Tshuva, E. Y.; Groysman, S.; Goldberg, I.; Kol, M.; Goldschmidt, Z. *Organometallics* **2002**, *21*, 662. (d) Groysman, S.; Goldberg, I.; Kol, M.; Genizi, E.; Goldschmidt, Z. *Organometallics* **2004**, *23*, 1880. (e) Groysman, S.; Tshuva, E. Y.; Goldberg, I.; Kol, M.; Goldschmidt, Z.; Shuster, M. *Organometallics* **2004**, *23*, 5291.

(12) Chan, M. C. W.; Tam, K. H.; Pui, Y. L.; Zhu, N. *J. Chem. Soc., Dalton Trans.* **2002**, 3085.

(13) Holligan, B. M.; Jeffery, J. C.; Norgett, M. K.; Schatz, E.; Ward, M. D. *J. Chem. Soc., Dalton Trans.* **1992**, 3345.

(14) Dietrich-Buchecker, C.; Sauvage, J. P. *Tetrahedron* **1990**, *46*, 503.

Table 1. Comparison of Selected Bond Lengths (Å) and Angles (deg) for 3, 4, and 7

	3	4	7
Zr1−N1	2.428(2)	2.407(4)	2.465(3)
Zr1−O1	1.954(2)	1.961(4)	1.967(2)
Zr1−O2	1.959(2)	1.960(4)	1.956(2)
Zr−Cl	2.427(1)	2.441(2)	2.520(1), 2.466(1), 2.437(1)
	2.439(1)	2.406(2)	
Zr−O(ketone)	2.206(2)	2.250(4)	
O1−Zr1−O2	156.3(1)	155.0(1)	157.8(1)
Cl1−Zr1−Cl2	96.14(4)	97.19(7)	93.17(4)

(ca. 6.0 to 7.0 ppm) and ^{31}P (−1.7 to −18.8 ppm) NMR spectra from the appearance of $^1J_{PH}$ coupling (488−526 Hz).

Crystal Structures: Comparison of Different Donor Groups. The molecular structures of complexes **3**, **4**, and **7** (Table 1 and Figure 1) have been determined by X-ray crystallography and can be compared with the previously reported structures of **1** and **2**.[12] The pyridine-2,6-bis(phenoxide) unit L^1 chelates to the distorted octahedral Zr core in **3**, **4**, and **7** in a tridentate meridional manner, and its nonplanarity is manifested in dihedral angles of ca. 40−50° between the aromatic rings. It is of interest to correlate the Zr−O(donor) bond lengths in these structures. The respective distances in **1**−**4** (2.247(3), 2.295(2), 2.206(2), and 2.250(4) Å) are elongated relative to that in the seminal metallocene cation $[Cp_2ZrMe(thf)]^+$ (2.122(14) Å)[15] but noticeably shorter than those in related catalysts such as Kol's amine-bis(aryloxide) derivative supported by a sidearm methoxy donor (Zr−OMe 2.447(3) Å)[11c] and Okuda's complexes bearing tridentate Cp-amido-methoxy donor ligands (Zr−OMe 2.330(4) and 2.375(2) Å).[16] The molecular structure of **7** confirms the anionic nature of the Zr moiety and the absence of a Zr−P interaction. The Zr−Cl bond lengths for the *trans* chloride groups (2.520(1) and 2.466(1) Å) are partially longer than for the *cis* chlorides in **3** and **4** (ca. 2.41−2.44 Å), presumably because these π-donors are competing for the same Zr d-orbital in the former case. Of course, *cis* configurations of the chloride ligands in these structures are important for their deployment as polyolefin catalysts. The crystal structure of the bis-ligand complex $[Zr(L^1)_2]$ has also been determined (see Supporting Information). The symmetric structure belongs to the tetragonal crystal system and the octahedral molecule is highly compact and spherical, which may explain the high tendency for its formation.

Polymerization Studies: Trends in Ethylene Polymerization. The **1**/MAO system displays excellent activities for ethylene polymerization, and an investigation into its catalytic characteristics was undertaken (Table 2). The highly active nature of **1** is illustrated by the appearance of exotherms (up to ∼60 °C) after ca. 3 min. Catalytic rates are noticeably reduced at 1 and 65 °C, although the latter may be influenced by diffusion-controlled factors. The polymerization efficiency of **1** is enhanced after the appearance of the exotherm (6 min: 7030 g mmol^{-1} h^{-1}), and an activity of 7880 g mmol^{-1} h^{-1} is observed using 2000 equiv of MAO, corresponding to a turnover frequency value of 2.81×10^5 h^{-1} atm^{-1}.

Polymer Characterization: Impact of Polymerization Conditions and Insight into Chain-Transfer Mechanism. GPC analysis of the polymer samples produced by **1**/MAO has been performed (Table 2 and Figure 2). In general, the materials exhibit low molecular weights (M_{pk} 1000−1800) and broad polydispersities (M_w/M_n 11−22; partly as a result of high MW tails). The exceptions are the polymers from the 1 (high MW and distinctly bimodal) and 65 (M_w/M_n 1.4) °C runs. ^{1}H and ^{13}C NMR spectroscopy has also been employed to characterize the polymers, all of which are highly linear polyethylene (see Supporting Information for examples). Saliently, only resonances for saturated methyl chain-end groups are observed (2.2−28.5 methyls per 1000 C), and the levels of vinyl hydrogens

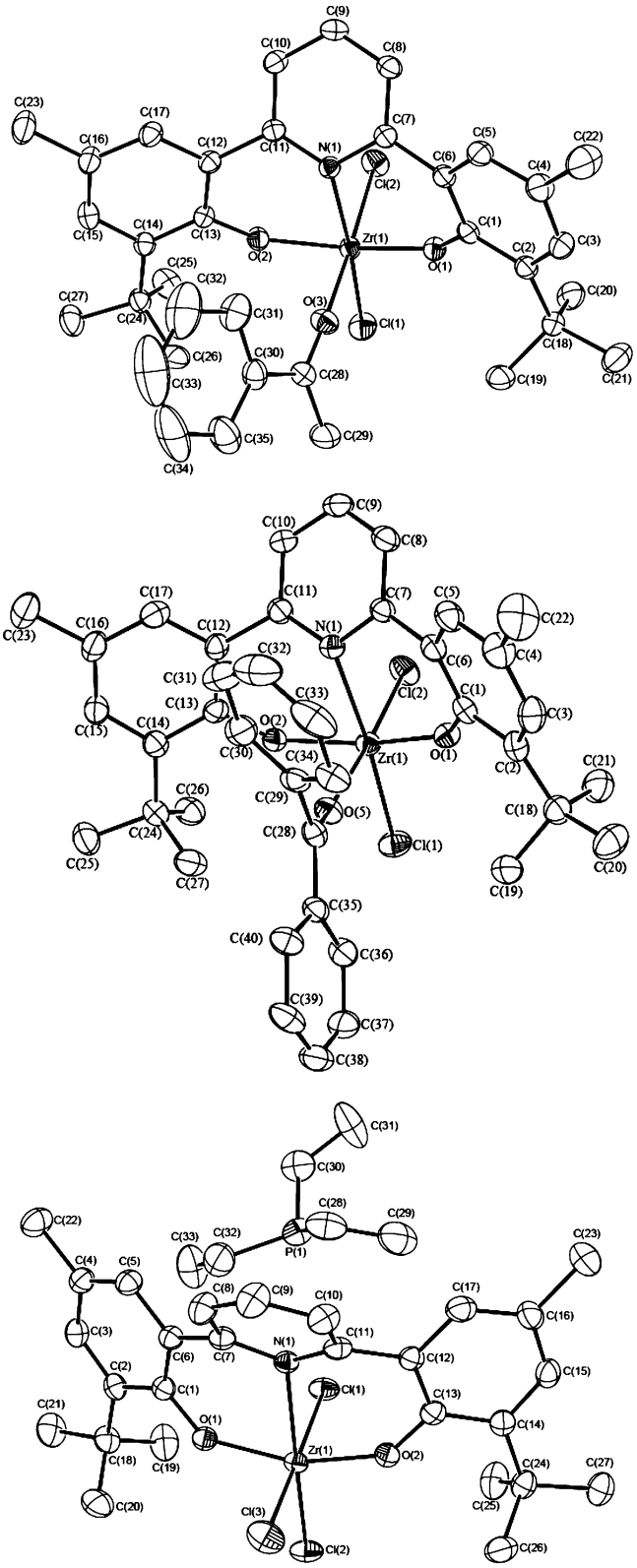

Figure 1. Perspective views of (from top) **3**, **4**, and **7** (30% probability ellipsoids).

(15) Jordan, R. F.; Bajgur, C. S.; Willett, R.; Scott, B. *J. Am. Chem. Soc.* **1986**, *108*, 7410.

(16) Amor, F.; Butt, A.; du Plooy, K. E.; Spaniol, T. P.; Okuda, J. *Organometallics* **1998**, *17*, 5836.

Table 2. Ethylene Polymerization Data for 1/MAO[a]

catalyst (μmol)	MAO (mmol/equiv)	temp (°C)	time (min)	yield (g)	activity[b]	T_m (°C)	M_w[c]	M_n[c]	M_w/M_n	M_{pk}[c]	chain-end gp[d] (methyl, vinyl)
4.72	4.72/1000	20	2	0.92	5850	129	46 000	2100	21.7	1800	11.6, 0
4.72	4.72/1000	1	2	0.23	1450	134	220 000	17 000	13.2	i: 24 000, ii: 432 000	2.2, 0[e]
4.72	4.72/1000	65	2	0.31	1990	111	1100	800	1.4	1000	28.5, 0[f]
4.72	4.72/1000	20	6[g]	3.32	7030	127	36 000	1800	19.8	1500	13.3, 0
3.15	6.30/2000	20	5[g]	2.44	7880	125	16 000	1400	11.4	1000	18.4, 0[e]

[a] Conditions: 50 mL of toluene, 1 atm pressure of ethylene. [b] Activity in g(polymer) (mmol catalyst)$^{-1}$ h^{-1}. [c] Determined by GPC at 135 °C using polyethylene standards. [d] Results from ^{13}C NMR analysis, given per 1000 carbon atoms. [e] Results from ^{1}H NMR analysis. [f] ^{1}H NMR analysis gave 29.6 methyl and 0.1 vinyl chain ends per 1000 carbon atoms. [g] An exotherm was observed.

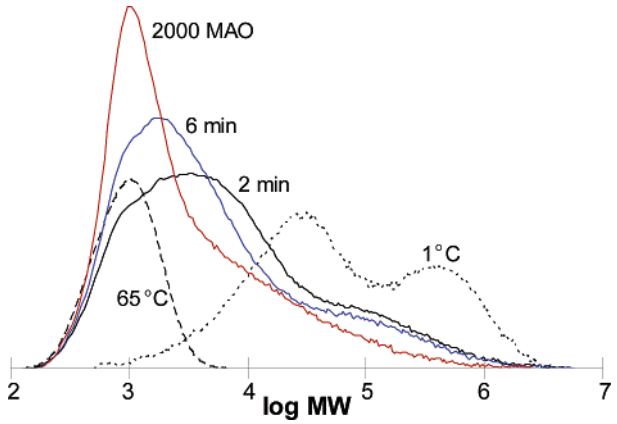

Figure 2. GPC traces of PE samples prepared by **1**/MAO (refer to Table 2).

corresponding to unsaturated chain ends are undetectable/negligible (or extremely low in the case of the 65 °C run). *With regard to the polymerization chain-transfer mechanism, the absence of unsaturated vinyl chain ends strongly indicates that the normally prevalent β-H transfer reactions to the metal or monomer are insignificant and signify that chain transfer to Al is vastly dominant.* It is interesting to note that the unusual chain transfer to Al pathway, which has been reported for group 4 metallocenes[17] and more recently for post-metallocene systems,[18,19] typically occurs concomitantly with β-H transfer and is rarely observed as the solitary chain-transfer process.[20,21]

The chain transfer to Al mechanism, which is dependent upon the alkyl Al concentration, can be invoked (rather than multiple active sites) to explain the broad polydispersities. Namely, the expected change in the concentration of Al species during polymerization would lead to a variable chain-transfer rate with time, and hence a broadening of the MW distribution. Furthermore, increasing the MAO concentration to 2000 equiv (Figure 2) has resulted in (1) a narrower M_w/M_n value, since changes in propagation and chain-transfer rates during polymerization are less significant for higher Al concentrations, and (2) lower MW material, as the chain-transfer rate to Al would increase to afford shorter polymer chains.

The GPC data imply that the rate of chain transfer to Al alters according to temperature (Table 2). At 1 °C, the chain-transfer rate is slow and high MW material is produced (see following section for explanation of bimodality). Higher temperatures should yield greater propagation and chain-transfer rates, culminating in enhanced activities and decreased MW, respectively (e.g., experiments accompanied by an exotherm display lower MW). At 65 °C, we suggest that the reduction in activity may partly be caused by the consumption of Al species at elevated chain-transfer rates. In addition, we note that the GPC and NMR data of the 65 °C run, especially the narrow polydispersity (1.4) and high level of saturated chain ends (~30 per 1000 C), show distinct similarities with those for the remarkably efficient "Fe-catalyzed polyethylene chain growth reaction on Zn" reported by Gibson and co-workers.[22]

Addition of Trimethylaluminum (TMA) to 1/MAO: Demonstrating Chain Transfer to Al. To gain further evidence for the chain transfer to Al pathway, we have studied the catalytic properties of **1**/MAO in the presence of varying amounts of TMA as chain-transfer agent and characterized the resultant polymer samples (Table 3). Polymerization conditions (0.5 °C, 100 equiv of MAO) have been carefully chosen to gave high MW materials in the absence of TMA, and the T_m values are clearly higher than for runs at 20 °C. Respectable activities are observed, and a downward trend is apparent for increasing TMA concentrations. While insoluble polymers are produced in the absence of and for 100 equiv of added TMA, the remaining materials have been analyzed by GPC (Figure 3). The polymer for 200 equiv of TMA is bimodal in nature, with a greater proportion in the higher MW fraction. For 500 equiv of TMA, the bimodality remains, but the lower MW fraction is now dominant. This trend is continued for 1000 equiv of TMA, where only the low MW portion at M_{pk} 11 000 is detected. Chain-end group analysis by ^{1}H NMR spectroscopy reveals saturated methyl fragments exclusively, the level of which consistently increases for higher TMA concentrations. None of the samples contained observable levels of hydrogens for unsaturated vinyl end groups. Furthermore, the samples exhibit a well-resolved triplet signal for the chain-end methyl group, suggesting that significant amounts of short chain branching is unlikely. *These observations are entirely consistent with chain transfer to Al as the sole chain-transfer mechanism during polymerization.*

The bimodal characteristics of the polymers are tentatively rationalized by the following: (1) the initial rate of chain transfer

(17) (a) Chien, J. C. W.; Wang, B.-P. *J. Polym. Sci. A* **1990**, *28*, 15. (b) Resconi, L.; Piemontesi, F.; Granciscono, G.; Abis, L.; Fiorani, T. *J. Am. Chem. Soc.* **1992**, *114*, 1025. (c) Mogstad, A.-L.; Waymouth, R. M. *Macromolecules* **1992**, *25*, 2282. (d) Leino, R.; Luttikhedde, H. J. G.; Lehmus, P.; Wilén, C.-E.; Sjöholm, R.; Lehtonen, A.; Seppälä, J. V.; Näsman, J. H. *Macromolecules* **1997**, *30*, 3477. (e) Byun, D.-J.; Kim, S. Y. *Macromolecules* **2000**, *33*, 1921.

(18) (a) Small, B. L.; Brookhart, M. Bennett, A. M. A. *J. Am. Chem. Soc.* **1998**, *120*, 4049. (b) Britovsek, G. J. P.; Bruce, M.; Gibson, V. C.; Kimberley, B. S.; Maddox, P. J.; Mastroianni, S.; McTavish, S. J.; Redshaw, C.; Solan, G. A.; Strömberg, S.; White, A. J. P.; Williams, D. J. *J. Am. Chem. Soc.* **1999**, *121*, 8728.

(19) (a) Murtuza, S.; Casagrande, O. L., Jr.; Jordan, R. F. *Organometallics* **2002**, *21*, 1882. (b) Michiue, K.; Jordan, R. F. *Macromolecules* **2003**, *36*, 9707. (c) Michiue, K.; Jordan, R. F. *Organometallics* **2004**, *23*, 460.

(20) (a) Scollard, J. D.; McConville, D. H.; Vittal, J. J.; Payne, N. C. *J. Mol. Catal. A* **1998**, *128*, 201. (b) Tsubaki, S.; Jin, J.; Sano, T.; Uozumi, T.; Soga, K. *Macromol. Chem. Phys.* **2001**, *202*, 1757.

(21) Saito, J.; Tohi, Y.; Matsukawa, N.; Mitani, M.; Fujita, T. *Macromolecules* **2005**, *38*, 4955.

(22) (a) Britovsek, G. J. P.; Cohen, S. A.; Gibson, V. C.; van Meurs, M. *J. Am. Chem. Soc.* **2004**, *126*, 9913. (b) van Meurs, M.; Britovsek, G. J. P.; Gibson, V. C.; Cohen, S. A. *J. Am. Chem. Soc.* **2005**, *127*, 9913.

Table 3. Polymerization Data for 1/MAO in the Presence of Trimethylaluminum (TMA)[a]

catalyst (μmol)	TMA (mmol/equiv)	Al/Zr	yield (g)	activity[b]	T_m (°C)	M_w[c]	M_n[c]	M_w/M_n	M_{pk}[c]	chain-end gp[e] (methyl, vinyl)
8.49	0	100	0.83	585	134			*d*		*f*
8.34	0.834/100	200	0.82	595	136			*d*		1.2, 0
8.18	1.636/200	300	0.53	390	137	668 000	26 000	25.7	i: 609 000, ii: 12 000	1.7, 0
8.02	4.010/500	600	0.28	205	136	261 000	9800	26.6	i: 13 000, ii: 568 000	3.2, 0
8.02	8.020/1000	1100	0.39	290	133	14 000	5400	2.5	11 000	*f*

[a] Conditions: 50 mL of toluene, 100 equiv of MAO, 1 atm pressure of ethylene, 0.5 °C, polymerization time 10 min. [b] Activity in g(polymer) (mmol catalyst)$^{-1}$ h^{-1}. [c] Determined by GPC at 135 °C using polyethylene standards. [d] Polymer was insoluble under analysis conditions. [e] Results from ^{1}H NMR analysis, given per 1000 carbon atoms. [f] Spectrum was too broad to allow integration.

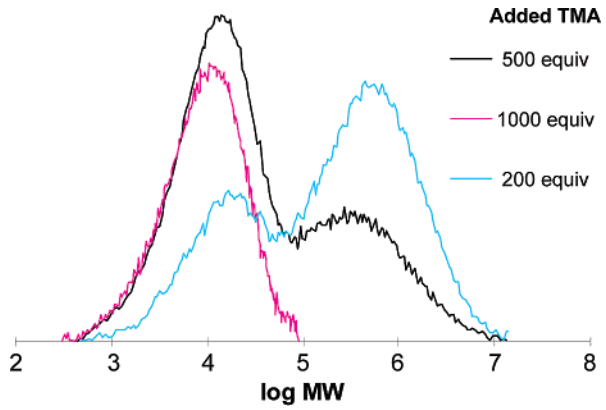

Figure 3. Addition of TMA to **1**/MAO: effects upon MW distribution (refer to Table 3).

to Al is highest and yields the lower MW fraction; (2) as the Al species is consumed and its concentration quickly depletes and becomes limiting, abrupt reduction in the rate of chain transfer to Al occurs and results in formation of the higher MW portion; (3) at 0.5 °C, the Al-chain-transfer rate can also drop as the catalyst becomes embedded in the polymer. Like the 2000 MAO experiment, the 1000 equiv of TMA run yields narrower polydispersity and a lower MW polymer. The general trend of declining activities at greater TMA concentrations can be attributed to coordination of TMA to the catalytically active species to generate [(L^1)ZrR(μ-Me)AlMe$_2$]$^+$, suppressing the propagation rate. The exception is the 1000 equiv of TMA run; we propose that enhancement of the chain-transfer rate at such high Al concentrations may overcompensate activity-wise for the diminishing effects of TMA coordination. Overall, the Al-chain-transfer characteristics of **1** appear to bear greater resemblance to the Ti diamide,[20] Fe pyridine-2,6-bis(imine),[18] and Zr bis(phenoxyimine)[21] catalysts rather than the Ti tris(pyrazolyl)borate[19] system. Namely, in the case of **1**, we believe that the dominance of the chain transfer to Al pathway is related to the creation of a highly accessible active site after loss of a labile donor group (see below), in a manner analogous to that reported for the Ti diamide system.[20]

Role of Donor Group. The excellent activities for the **1**/MAO system are intriguing given the presence of the thf ligand at the oxophilic Zr(IV) center. This is in stark contrast to the well-established suppression in catalytic efficiency for the solvated [Cp$_2$ZrMe(L)]$^+$ cations (L = thf, amine).[23] Reduced activities for the living polymerization of 1-hexene by coordinatively unsaturated chelating diamide Ti(IV) derivatives have been attributed to binding of the toluene solvent at the cationic active site,[24] while thf-solvated Sc(III) complexes bearing related β-diketiminato ligands have been isolated.[25] Nevertheless, highly active polyethylene catalysts derived from cationic iron and cobalt pyridine-2,6-bis(imino) complexes bearing thf and CH$_3$CN donors have been described.[26] In this work, we have prepared a series of Zr(IV) catalysts containing different O-donors and Cl[HPR$_3$] fragments, and comparative polymerization experiments have been carried out simultaneously using the same batch of MAO in order to probe the role of the donor group and ascertain whether the donor remains bound to the Zr core during catalysis and replaces the function of the "sidearm donor" reported by Kol.[11]

Although variations in the activities of **1**−**8** are observed (Table 4), differences within the respective ketone and Cl[HPR$_3$] series are also evident, and no distinct trends are apparent. Characterizations of the polymer samples are more informative: the T_m values of all materials fall within a narrow range. GPC analysis of **1**−**5** (Figure 4) reveals low MW materials, the properties and profiles of which are very similar (e.g., M_w/M_n 3.7−4.5). ^{1}H NMR analysis also indicates that the polymers obtained from **1**−**5** are comparable, and the levels of methyl chain-end groups correspond closely (11.8−13.2 methyls per 1000 C). Like in Tables 2 and 3, none of the samples exhibit resonances for vinyl hydrogens, which signifies the absence of unsaturated chain ends and the dominance of the chain transfer to Al pathway (over β-H transfer). On the basis of Table 4 and the polymer characterization data, we propose that (1) the influence of the donor group during polymerization is minimal, (2) the same active species (i.e., [(L^1)ZrR]$^+$) is generated by **1**−**8**/MAO, and (3) the donor group is sequestered by the MAO cocatalyst[26] and does not actively participate in the polymerization reaction. We attribute the apparent differences in activities for **1**−**8** to slight variations in catalyst as well as Al concentrations in each run, while the initiation period for each catalyst may also fluctuate.

Homo- and Copolymerization Studies on 1 with Different Cocatalysts. Catalyst **1** was selected for large-scale ethylene polymerization and copolymerization experiments with propylene and norbornene using MAO or ^{i}Bu$_3$Al/Ph$_3$CB(C$_6$F$_5$)$_4$ as the cocatalyst (Table 5). For ethylene polymerization, an excellent activity of 5700 g mmol^{-1} h^{-1} is observed for **1**/MAO (considering the Al/Zr ratio is only 250), although the **1**/^{i}Bu$_3$Al/Ph$_3$CB(C$_6$F$_5$)$_4$ system displays a substantially superior activity of 36 590 g mmol^{-1} h^{-1} (at a reduced catalyst concentration). In general, the use of the ^{i}Bu$_3$Al/borate cocatalyst leads to elevated homo- and copolymerization activities and slightly lower MW materials.

(23) Jordan, R. F. *Adv. Organomet. Chem.* **1991**, *32*, 325.
(24) Scollard, J. D.; McConville, D. H. *J. Am. Chem. Soc.* **1996**, *118*, 10008.
(25) (a) Lee, L. W. M.; Piers, W. E.; Elsegood, M. R. J.; Clegg, W.; Parvez, M. *Organometallics* **1999**, *18*, 2947. (b) Hayes, P. G.; Piers, W. E.; R. McDonald, *J. Am. Chem. Soc.* **2002**, *124*, 2132.
(26) Britovsek, G. J. P.; Gibson, V. C.; Spitzmesser, S. K.; Tellman, K. P.; White, A. J. P.; Williams, D. J. *J. Chem. Soc., Dalton Trans.* **2002**, 1159.

Table 4. Comparison of Ethylene Polymerization Data for Catalysts Bearing Different Donor Groups[a]

catalyst (μmol)	yield (g)	activity[b]	T_m (°C)	M_w [c]	M_n [c]	M_w/M_n	M_{pk} [c]	chain-end gp[e] (methyl, vinyl)
1 (5.66)	0.97	3450	126	8000	2000	4.0	1800	13.2, 0
2 (5.66)	0.70	2580	127	9700	2100	4.5	1700	12.0, 0
3 (5.76)	0.71	2050	126	7600	2000	3.7	1800	12.6, 0
4 (5.70)	0.52	2010	130	8000	2200	3.7	1800	12.8, 0
5 (5.86)	0.98	2990	127	8200	2100	3.9	1900	11.8, 0
6 (5.78)	1.03	3535	125			*d*		*d*
7 (5.72)	0.82	3170	126			*d*		*d*
8 (5.70)	0.94	3215	125			*d*		*d*

[a] Conditions: 35 mL of toluene, 1000 equiv of MAO, 1 atm pressure of ethylene, 20 °C, polymerization time 3 min. [b] The reported activity, in g(polymer) (mmol catalyst)$^{-1}$ h^{-1}, is the mean value of 3 separate sets of polymerization runs for **1**−**8** using the same batch of MAO. [c] Determined by GPC at 135 °C using polyethylene standards. [d] Not recorded. [e] Results from ^{1}H NMR analysis, given per 1000 carbon atoms.

Table 5. Homo- and Copolymerization Results for 1[a]

	reaction	yield (g)	activity[b]	M_v [c]	notes
1/MAO	PE	2.37	5700	8.03×10^5	T_m 137 °C
	EPR	0.89	2150	3.29×10^5	<5 mol % C3[e]
	COC	0.44	530	4.50×10^5	T_m 132 °C
1/^{i}Bu$_3$Al/Ph$_3$CB(C$_6$F$_5$)$_4$	PE	3.05[d]	36 590	1.93×10^5	T_m 134 °C
	EPR	6.54	15 700	2.21×10^4	25.4 mol % C3[f]
	COC	3.32	7970	1.83×10^5	T_m 130 °C

[a] Conditions: 250 mL of toluene, 5 μmol of catalyst, cocat. MAO (250 equiv) or ^{i}Bu$_3$Al/Ph$_3$CB(C$_6$F$_5$)$_4$ (50/1.2 equiv, respectively, vs **1**), 1 atm olefin feed, 25 °C, PE (ethylene polymerization, 5 min): C2 = 100 L h^{-1}, EPR (ethylene−propylene copolymerization, 5 min): C2/C3 = 100/100 L h^{-1}, COC (ethylene−norbornene copolymerization, 10 min): C2 = 50 L h^{-1} and NB = 1 g. [b] Activity in g(polymer) (mmol catalyst)$^{-1}$ h^{-1}. [c] Determined by intrinsic viscosity [η] of polymer at 135 °C in decalin and calculated using [η] = $6.2 \times 10^{-4} M_v^{0.7}$. [d] 1 μmol of catalyst. [e] Estimated by IR analysis (polymer was insoluble under ^{1}H NMR analysis conditions). [f] Determined by ^{1}H NMR analysis.

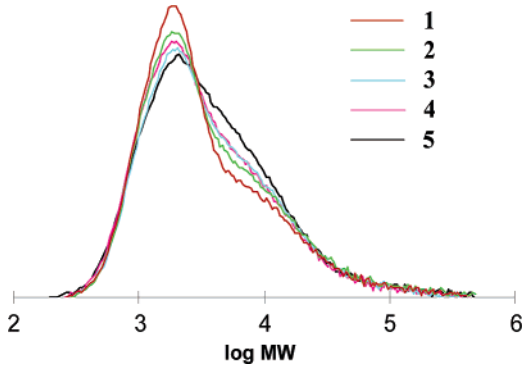

Figure 4. GPC traces of PE samples prepared by **1**−**5**/MAO (refer to Table 4).

Notable results have been obtained in ethylene−propylene copolymerization reactions.[27] The **1**/^{i}Bu$_3$Al/Ph$_3$CB(C$_6$F$_5$)$_4$ system exhibits an impressive activity of 15 700 g mmol^{-1} h^{-1}, and a poly(ethylene-*co*-propylene) (EPR) material with good C3 content (25.4 mol % C3) is produced. The activity and degree of C3 incorporation can be compared with the performance of the Zr bis(phenoxyimine)/MAO and -/^{i}Bu$_3$Al/Ph$_3$CB(C$_6$F$_5$)$_4$ systems and that of Cp$_2$ZrCl$_2$/MAO (22 000, 600−8000, and 22 000 g mmol^{-1} h^{-1}, respectively; 10.1, 20.7−23.7, and 25.6 mol % C3, respectively) under similar conditions,[3a,28] although the level of C3 incorporation is clearly inferior to that of Me$_2$X(3-RCp)(9-Flu)ZrCl$_2$/MAO (>50 mol % C3; X = C, Si; R = Me, ^{i}Pr).[27d] In contrast, the **1**/MAO system yields decreased activities and very low C3 content, the latter indicated by IR analysis and the appearance of T_m (132 °C) for the resultant polymer. Both **1**/MAO and **1**/^{i}Bu$_3$Al/Ph$_3$CB(C$_6$F$_5$)$_4$ exhibit poor NB incorporation in ethylene−norbornene copolymerization, as implied by the high PE-like T_m values. We note that Fujita et al. have investigated the contrasting effects of the MAO and ^{i}Bu$_3$Al/Ph$_3$CB(C$_6$F$_5$)$_4$ cocatalysts upon the reactivity of bis(phenoxyimine) Zr catalysts, with the latter showing suppressed activities.[3a,29] The reasons for the reversal of this trend for catalyst **1** and the superior performance of the **1**/^{i}Bu$_3$Al/Ph$_3$CB(C$_6$F$_5$)$_4$ system are currently unclear, although at high Al/MAO levels, it is apparent that the coordination of Al species to the catalytic site may reduce activities.

Concluding Remarks

Despite reports regarding the poor catalytic activities of group 4 complexes supported by tridentate amine-bis(aryloxide) ligands, we have established that the related pyridine-2,6-bis(aryloxide) Zr system can exhibit exceptional activities for olefin polymerization. Compared to aliphatic alkoxide analogues, the tridentate pyridine-2,6-bis(aryloxide) moiety is a rigid and chemically inert ligand framework and is expected to be more resistant to alkyl aluminum-induced catalyst decomposition and rearrangement reactions. It is also pertinent to refer to calculations by Musaev and Morokuma[30] on the related 2,2′-thio-bis(4-methyl-6-*tert*-butylphenoxide) Ti complexes,[7,9] which predicted that strong binding by the central chelating unit in tridentate [O,L,O] catalysts, like the pyridine group in [Zr(L^1)Cl$_2$(thf)] (**1**), would lead to lower ethylene insertion barriers and hence enhanced activities.

Several of the [Zr(L^1)Cl$_2$(donor)] derivatives have been structurally characterized, and the importance of the donor group with respect to complex formation, isolation, and solubility has been indicated. Careful investigation of the behavior of catalysts

(27) (a) Kravchenko, R.; Waymouth, R. M. *Macromolecules* **1998**, *31*, 1. (b) Galimberti, M.; Piemontesi, F.; Mascellani, N.; Camurati, I.; Fusco, O.; Destro, M. *Macromolecules* **1999**, *32*, 7968. (c) Wang, W.-J.; Zhu, S.; Park, S.-J. *Macromolecules* **2000**, *33*, 5770. (d) Fan, W.; Leclerc, M. K.; Waymouth, R. M. *J. Am. Chem. Soc.* **2001**, *123*, 9555.

(28) Ishii, S.; Saito, J.; Matsuura, S.; Suzuki, Y.; Furuyama, R.; Mitani, M.; Nakano, T.; Kashiwa, Fujita, T. *Macromol. Rapid Commun.* **2002**, *23*, 693.

(29) Makio, H.; Fujita, T. *Bull. Chem. Soc. Jpn.* **2005**, *78*, 52.

(30) (a) Froese, R. D. J.; Musaev, D. G.; Matsubara, T.; Morokuma, K. *J. Am. Chem. Soc.* **1997**, *119*, 7190. (b) Froese, R. D. J.; Musaev, D. G.; Morokuma, K. *Organometallics* **1999**, *18*, 373. (c) Vyboishchikov, S. F.; Musaev, D. G.; Froese, R. D. J.; Morokuma, K. *Organometallics* **2001**, *20*, 309.

bearing different O-donors and Cl[HPR$_3$] groups and analysis of the resultant polymers suggest that a single active species is responsible and the donor group is unlikely to perform an active role during the polymerization process. While the activity of **1**/MAO is among the highest reported for non-Cp aryloxide or alkoxide derivatives at such MAO concentrations, the best activities in this work are reserved for the **1**/^{i}Bu$_3$Al/Ph$_3$CB(C$_6$F$_5$)$_4$ system. Catalytic efficiencies of 36 590 and 15 700 g mmol^{-1} h^{-1} are observed for ethylene polymerization and ethylene−propylene copolymerization, respectively, with the latter incorporating a respectable degree of propylene (25.4 mol %). The polymerization characteristics of **1**/MAO have been studied by modification of reaction conditions such as temperature, time, and particularly Al concentration (with MAO cocatalyst and TMA chain-transfer agent). Polymer characterization by GPC and ^{1}H and ^{13}C NMR spectroscopy clearly signifies that **1**/MAO constitutes a rare catalytic system where the conventional β-H transfer processes to the metal/monomer are shut down and the chain-transfer mechanism is overwhelmingly (or exclusively) dominated by chain transfer to Al.

Experimental Section

General Considerations. All reactions were performed under a nitrogen atmosphere using standard Schlenk techniques or in a Braun drybox. All solvents were appropriately dried and distilled, then degassed prior to use. ^{1}H and ^{13}C NMR spectra were recorded on a Bruker 500 DRX, 400 DRX, or 300 FT-NMR spectrometer (ppm) using Me$_4$Si as internal standard. ^{31}P NMR spectra were recorded on the Bruker 400 DRX and referenced to external 85% H$_3$PO$_4$. Peak assignments were based on combinations of DEPT-135 and 2-D ^{1}H−^{1}H, ^{13}C−^{1}H, and NOE correlation NMR experiments. Mass spectra (EI) were obtained on a Finnigan MAT 95 mass spectrometer. Elemental analyses were performed by Medac Ltd., UK. For polymer analysis, melting points were determined by differential scanning calorimetry on a Perkin-Elmer DSC7. ^{1}H and ^{13}C NMR data for polymer samples were obtained in *p*-xylene-d_{10} at 110 °C and 1,2,4-trichlorobenzene/C$_2$D$_2$Cl$_4$ at 130 °C, respectively. Gel permeation chromatographs were obtained on a Waters 150CV [columns supplied by Shodex (807, 806, and 804)] at 135 °C using polyethylene standard reference material NBS1484a. Methylaluminoxane (MAO, 10 wt % solution in toluene) was purchased from Aldrich and used as received. Ethylene (BOC, polymer grade) was passed through Drierite and P$_2$O$_5$. By following the synthetic procedure for Zr(CH$_2$Ph)$_2$Cl$_2$(OEt$_2$)$_2$,[31] the complex Zr(CH$_2$Ph)$_2$Cl$_2$(OEt$_2$)(dioxane)$_{0.5}$ was isolated as an orange crystalline solid and characterized by ^{1}H NMR spectroscopy to contain the O-donor ligands in the stoichiometry shown. Zr(CH$_2$Ph)$_4$ was prepared according to the published method.[32] The syntheses of ligand H$_2$L^1 and complexes **1** and **2** were previously given.[12]

Improved Synthesis of [Zr(L^1)Cl$_2$(thf)] (1). A solution of H$_2$L^1 (0.345 g, 0.86 mmol) in toluene (15 mL) and THF (8 mL) was slowly added at −78 °C to Zr(CH$_2$Ph)$_2$Cl$_2$(OEt$_2$)(dioxane)$_{0.5}$ (0.400 g, 0.86 mmol) in toluene (15 mL) and THF (8 mL). The resultant yellow solution was stirred for 1 h at −78 °C and for 12 h at room temperature. Filtration and concentration of this mixture gave a pale yellow solid, which was recrystallized from toluene to yield large yellow crystals. Yield: 0.45 g, 77%. All characterization data were identical to those previously reported.

[Zr(L^1)$_2$] was isolated as the major product from the original reaction procedure (slow addition of Li$_2$L^1 to ZrCl$_4$ in toluene at −78 °C)[12] if the addition of Li$_2$L^1 was accelerated or in the absence of a suitable donor solvent/ligand (e.g., THF). Data for [Zr(L^1)$_2$]: ^{1}H NMR (300 MHz, C$_6$D$_6$): 1.13 (s, 18H, ^{t}Bu), 2.32 (s, 6H, Me), 7.18−7.23 (m, 1H, py-H^4), 7.25 (s, 2H, Ar), 7.33−7.36 (m, 4H, py-H^{3,5} and Ar). ^{13}C NMR (75 MHz, C$_6$D$_6$): 21.18 (Me), 29.61 (C*Me$_3$*), 34.83 (*C*Me$_3$); methine carbons: 123.26, 128.93, 130.50, 139.08; 4° carbons: 125.76, 126.63, 138.18, 156.52, 156.80. EI-MS (+ve, *m*/*z*): 894 (100%) [M$^+$].

General Synthetic Procedure for Complexes 3−8. A solution of H$_2$L^1 (0.200 g, 0.50 mmol) in toluene (35 mL) was slowly added at −78 °C to Zr(CH$_2$Ph)$_2$Cl$_2$(OEt$_2$)(dioxane)$_{0.5}$ (0.246 g, 0.53 mmol) in toluene (25 mL) in the presence of excess ketone (5−10 mmol) or phosphine (ca. 20 mmol). The resultant pale yellow solution was stirred for 1 h at −78 °C and for 12 h at room temperature. Filtration and concentration of this mixture gave a pale yellow solid, which was recrystallized from toluene to yield yellow crystals.

[Zr(L^1)Cl$_2$(O=CPhMe)] (3). Acetophenone (1 mL, 8.6 mmol) was used. Yield: 0.22 g, 61%. ^{1}H NMR (400 MHz, CD$_2$Cl$_2$): 1.43 (s, 18H, ^{t}Bu), 2.32 (s, 6H, Me), 2.47 (br, 3H, MeC=O), 7.13 (s, 2H, Ar), 7.18 (s, 2H, Ar), 7.32 (br, 2H, PhC=O), 7.62 (t, 1H, J = 7.4 Hz), 7.67 (br, 2H, PhC=O), 7.84 (d, J = 7.9 Hz, 2H, py-H^{3,5}), 8.07 (t, J = 7.9 Hz, 1H, py-H^4). ^{13}C NMR (126 MHz, CD$_2$Cl$_2$): 20.9 (MeC=O), 29.7 (C*Me$_3$*), 35.0 (*C*Me$_3$); methine carbons: 124.3, 129.0, 129.8, 130.0, 130.9, 137.1, 140.7; 4° carbons: 127.7, 129.3, 137.5, 154.1, 160.0. EI-MS (+ve, *m*/*z*): 563 (100%) [M$^+$ − PhC(O)Me]. Anal. Calcd for C$_{35}$H$_{39}$NO$_3$Cl$_2$Zr·0.5C$_7$H$_8$ (729.90): C, 63.35; H, 5.94; N, 1.92. Found: C, 63.08; H, 5.93; N, 1.78.

[Zr(L^1)Cl$_2$(O=CPh$_2$)] (4). Benzophenone (1.8 g, 9.9 mmol) was used. Yield: 0.26 g, 65%. ^{1}H NMR (400 MHz, CD$_2$Cl$_2$): 1.44 (s, 18H, ^{t}Bu), 2.30 (s, 6H, Me), 6.93 (s, 2H, Ar), 7.15 (s, 2H, Ar), 7.24 (br m, 4H, Ph$_2$C=O), 7.53 (br m, 4H, Ph$_2$C=O), 7.57 (br m, 2H, Ph$_2$C=O), 7.60 (d, J = 7.9 Hz, 2H, py-H^{3,5}), 7.85 (t, J = 7.8 Hz, 1H, py-H^4). ^{13}C NMR (126 MHz, CD$_2$Cl$_2$): 20.9 (Me), 29.8 (C*Me$_3$*), 35.0 (*C*Me$_3$); methine carbons: 123.9, 128.4, 129.7, 129.8, 132.6, 135.3, 140.2; 4° carbons: 127.7, 129.1, 137.4, 153.9, 159.7. EI-MS (+ve, *m*/*z*): 563 (100%) [M$^+$ − Ph$_2$C=O]. Anal. Calcd for C$_{40}$H$_{41}$NO$_3$Cl$_2$Zr (745.90): C, 64.41; H, 5.54; N, 1.88. Found: C, 64.79; H, 5.29; N, 2.04.

[Zr(L^1)Cl$_2$(O=CNpMe)] (5). 2-Acetonaphthone (NpC(O)Me, 0.84 g, 4.9 mmol) was used. Yield: 0.24 g, 62%. ^{1}H NMR (400 MHz, CD$_2$Cl$_2$): 1.44 (s, 18H, ^{t}Bu), 2.31 (s, 6H, Me), 2.59 (br, 3H, MeC=O), 7.15 (s, 2H, Ar), 7.16 (s, 2H, Ar), 7.56 (t, J = 7.2 Hz, 1H, Np), 7.58 (br, 1H, Np), 7.67 (t, J = 7.6 Hz, 1H, Np), 7.70 (br, 1H, Np), 7.80 (br, 2H, Np), 7.85 (d, J = 7.9 Hz, 2H, py-H^{3,5}), 8.07 (t, J = 7.9 Hz, 1H, py-H^4), 8.35 (br, 1H, Np). ^{13}C NMR (126 MHz, CD$_2$Cl$_2$): 20.9 (Me), 29.8 (C*Me$_3$*), 35.0 (*C*Me$_3$); methine carbons: 124.3, 124.4, 127.6 (br), 128.0, 128.9 (br), 129.8, 130.0, 130.6 (br), 131.0 (br), 135.0 (br), 140.7; 4° carbons: 127.7, 129.3, 137.6, 154.2, 160.1. EI-MS (+ve, *m*/*z*): 563 (100%) [M$^+$ − NpC(O)Me]. Anal. Calcd for C$_{39}$H$_{41}$NO$_3$Cl$_2$Zr (733.89): C, 63.83; H, 5.63; N, 1.91. Found: C, 63.65; H, 5.63; N, 1.96.

[Zr(L^1)Cl$_3$][HPMe$_3$] (6). Trimethylphosphine (3 mL, 29 mmol) was used. Yield: 0.21 g, 57% yield. ^{1}H NMR (400 MHz, CD$_2$Cl$_2$): 1.54 (s, 18H, ^{t}Bu), 1.78 (dd, J = 15.2, 4.5 Hz, 9H, PC*H$_3$*), 2.30 (s, 6H, Me), 6.14 (br virtual s, HP), 7.08 (s, 2H, Ar), 7.22 (s, 2H, Ar), 7.73 (d, J = 7.9 Hz, 2H, py-H^{3,5}), 7.97 (t, J = 7.9 Hz, 1H, py-H^4). ^{13}C NMR (126 MHz, CD$_2$Cl$_2$): 5.8 (d, $^1J_{PC}$ = 54 Hz, P*C*H$_3$), 20.6 (Me), 29.8 (C*Me$_3$*), 34.7 (*C*Me$_3$); methine carbons: 123.7, 129.2, 129.5, 139.6; 4° carbons: 127.6, 127.8, 136.6, 154.5, 159.2. ^{31}P[^{1}H] NMR (CD$_2$Cl$_2$): −4.90 (d, $^1J_{PH}$ = 511 Hz). EI-MS (+ve, *m*/*z*): 563 (100%) [M$^+$ − (PMe$_3$H)Cl]. Anal. Calcd for C$_{30}$H$_{41}$NO$_2$Cl$_3$PZr (676.21): C, 53.29; H, 6.11; N, 2.07. Found: C, 53.37; H, 6.00; N, 2.26.

[Zr(L^1)Cl$_3$][HPEt$_3$] (7). Triethylphosphine (3 mL, 20.3 mmol) was used. Yield: 0.23 g, 60%. ^{1}H NMR (400 MHz, CD$_2$Cl$_2$): 1.21 (dt, J = 19.9, 7.7 Hz, 9H, PCH$_2$C*H$_3$*), 1.55 (s, 18H, ^{t}Bu), 2.18 (br m, 6H, PC*H$_2$*CH$_3$), 2.33 (s, 6H, Me), 6.48 (br d, $^1J_{PH}$ = 488 Hz, 1H, HP), 7.09 (s, 2H, Ar), 7.22 (s, 2H, Ar), 7.73 (d, J = 7.9 Hz,

(31) Wengrovius, J. H.; Schrock, R. R. *J. Organomet. Chem.* **1981**, *205*, 319.

(32) Zucchini, U.; Albizzati, E.; Giannini, U. *J. Organomet. Chem.* **1971**, *26*, 357.

2H, py-H^{3,5}), 7.97 (t, J = 7.9 Hz, 1H, py-H^4). ^{13}C NMR (126 MHz, CD_2Cl_2): 6.4 (br s, PCH_2CH_3), 9.9 (d, $^1J_{PC}$ = 48 Hz, PCH_2CH_3), 20.6 (Me), 29.7 (CMe_3), 34.7 (CMe_3); methine carbons: 123.7, 129.1, 129.4, 139.4; 4° carbons: 127.6, 136.6, 154.6, 159.2. ^{31}P NMR (CD_2Cl_2): −18.78. EI-MS (+ve, *m*/*z*): 563 (100%) [M^+ − (PEt_3H)Cl]. Anal. Calcd for $C_{33}H_{47}NO_2Cl_3PZr$ (718.29): C, 55.18; H, 6.59; N, 1.95. Found: C, 55.36; H, 6.46; N, 1.60.

[Zr(L^1)Cl$_3$][HPMe$_2$Ph] (8). Dimethylphenylphosphine (3 mL, 21.1 mmol) was used. Yield: 0.22 g, 56% yield. ^{1}H NMR (400 MHz, $CDCl_3$): 1.54 (s, 18H, ^{t}Bu), 2.03 (br, 6H, PCH_3), 2.33 (s, 6H, Me), 7.09 (s, 2H, Ar), 7.22 (s, 2H, Ar), 7.58 (br, 2H, PhP), 7.68 (br, 3H, PhP), 7.74 (d, J = 7.9 Hz, 2H, py-H^{3,5}), 7.98 (t, J = 7.9 Hz, 1H, py-H^4). ^{13}C NMR (126 MHz, $CDCl_3$): 20.6 (Me), 29.1 (PCH_3; $^1J_{PC}$ coupling obscured by CMe_3 peak), 29.7 (CMe_3), 34.7 (CMe_3); methine carbons: 120.1 (br), 123.7, 126.2 (br), 129.2, 129.5, 131.4 (br), 139.5; 4° carbons: 127.6, 127.7, 136.6, 154.6, 159.3. ^{31}P[^{1}H] NMR (CD_2Cl_2): −1.73 (d, $^1J_{PH}$ = 526 Hz). EI-MS (+ve, *m*/*z*): 563 (100%) [M^+ − (PMe_2PhH)Cl]. Anal. Calcd for $C_{35}H_{43}NO_2Cl_3PZr$ (738.28): C, 56.94; H, 5.87; N, 1.90. Found: C, 56.72; H, 5.80; N, 1.95.

[Zr(L^1)(CH$_2$Ph)$_2$] (9). A solution of H_2L^1 (0.230 g, 0.57 mmol) in diethyl ether (15 mL) was slowly added to $Zr(CH_2Ph)_4$ (0.260 g, 0.57 mmol) in diethyl ether (15 mL) at −78 °C. The resultant mixture was stirred for 30 min at −78 °C and for 10 h at room temperature to give a bright yellow cloudy solution. Concentration and storage of the solution at −78 °C for 12 h gave a bright yellow crystalline solid. Yield: 0.24 g, 62%. ^{1}H NMR (400 MHz, C_6D_6): 1.74 (s, 18H, ^{t}Bu), 2.27 (s, 6H, Me), 2.67 (s, 4H, CH_2), 6.56 (t, J = 7.3 Hz, 2H, *p*-Ph), 6.76 (m, 6H, *m*-Ph and Ar−H^6), 6.80 (t, J = 7.6 Hz, 1H, py-H^4), 6.92 (d, J = 7.8 Hz, 2H, py-H^{3,5}), 7.00 (d, J = 7.3 Hz, 4H, *o*-Ph), 7.35 (s, 2H, Ar−H^4). ^{13}C NMR (126 MHz, C_6D_6): 21.17 (Me), 30.74 (CMe_3), 35.37 (CMe_3), 59.53 (CH_2, $^1J_{CH}$ = 134.5 Hz), 123.43 (*p*-Ph), 124.68 (py-C^{3,5}), 129.51 (*o*-Ph), 129.80 (*m*-Ph), 130.10 (Ar-C^4), 130.59 (Ar-C^6), 138.49 (py-C^4); 4° carbons: 127.77, 128.56, 136.52, 138.16, 154.78, 159.62. Anal. Calcd for $C_{41}H_{45}NO_2Zr$ (675.04): C, 72.95; H, 6.72; N, 2.07. Found: C, 73.03; H, 6.42; N, 2.14.

X-ray Crystallography. Crystals mounted in a glass capillary were used for data collection at −20 °C on a MAR diffractometer with a 300 mm image plate detector using graphite-monochromatized Mo Kα radiation (λ = 0.71073 Å). Data collection was made with 2° oscillation steps of φ, 420 s exposure time, and scanner distance at 120 mm, and 100 images were collected. The images were interpreted and intensities integrated using the program DENZO, and the structure was solved by direct methods employing the SIR-97 program on a PC.[33] For **3**: $C_{35}H_{39}Cl_2NO_3Zr\cdot C_6D_6$, fw = 767.98, monoclinic, $P2_1/n$, a = 15.432(3) Å, b = 16.281(3) Å, c = 17.126(3) Å, β = 115.36(3)°, V = 3888.2(12) Å^3, Z = 4, D_c = 1.312 g cm^{-3}, μ(Mo Kα) = 0.457 mm^{-1}, F(000) = 1584, T = 253(2) K, $2\theta_{max}$ = 50.7°, h −18 to 18; k −19 to 19; l −18 to 18, 6301 indep reflns (R_{int} = 0.0468), 433 variable parameters, R_1 = 0.036 ($I > 2\sigma(I)$), wR_2 = 0.092, GOF(F^2) = 0.986, largest diff peak/hole = 0.38/−0.46 e Å^{-3}. For **4**: $C_{40}H_{41}NO_3Cl_2Zr\cdot(C_7H_8)_{0.25}$, fw = 768.93, triclinic, $P\bar{1}$ (#2), a = 10.743(2) Å, b = 18.631(4) Å, c = 19.868(4) Å, α = 81.32(3)°, β = 81.24(3)°, γ = 78.01(3)°, V = 3815.1(13) Å^3, Z = 4, D_c = 1.339 g cm^{-3}, μ(Mo Kα) = 0.467 mm^{-1}, F(000) = 1594, T = 253(2) K, $2\theta_{max}$ = 50.7°, h −11 to 11; k −22 to 22; l −22 to 23, 10554 indep reflns (R_{int} = 0.0515), 863 variable parameters, R_1 = 0.057 ($I > 2\sigma(I)$), wR_2 = 0.142, GOF(F^2) = 0.960, largest diff peak/hole = 0.79/−0.48 e Å^{-3}. For **7**: $C_{33}H_{47}NO_2Cl_3PZr$, fw = 718.29, monoclinic, $P2_1/n$, a = 12.324(3) Å, b = 17.074(3) Å, c = 17.421(4) Å, β = 96.72(3)°, V = 3640.5(13) Å^3, Z = 4, D_c = 1.310 g cm^{-3}, μ(Mo Kα) = 0.594 mm^{-1}, F(000) = 1496, T = 253(2) K, $2\theta_{max}$ = 50.7°, h −14 to 14; k −20 to 19; l −18 to 20, 6117 indep reflns (R_{int} = 0.0375), 381 variable parameters, R_1 = 0.041 ($I > 2\sigma(I)$), wR_2 = 0.104, GOF(F^2) = 0.998, largest diff peak/hole = 0.85/−0.65 e Å^{-3}.

Polymerization Procedures. Schlenk-line ethylene polymerization runs were carried out under atmospheric pressure in toluene in a 100 mL glass reactor containing a magnetic stir bar. The stirred solution containing the catalyst was thermostated to the required temperature and purged with ethylene for 15 min. Polymerization was initiated by adding a toluene solution of methylaluminoxane (MAO), and the reactor was maintained under 1 atm of ethylene for the duration of the polymerization. After the prescribed time, HCl-acidified methanol (40 mL) was added to terminate the polymerization, and the ethylene gas feed was stopped. The resultant solid polymer was collected by filtration, washed with acidified methanol, and dried under vacuum at 80 °C for 12 h.

Large-scale ethylene polymerization tests were carried out under atmospheric pressure in toluene in a 500 mL glass reactor equipped with a propeller-like stirrer. Toluene (250 mL) was introduced into the nitrogen-purged reactor and stirred (600 rpm). The toluene was thermostated to 25 °C, and the ethylene gas feed (100 L/h) was then started. After 15 min, polymerization was initiated by adding toluene solutions of the cocatalyst, then catalyst, into the reactor with vigorous stirring (600 rpm). After the prescribed time, isobutyl alcohol (10 mL) was added to terminate the polymerization, and the ethylene gas feed was stopped. To the resulting mixture were added methanol (1000 mL) and concentrated HCl (2 mL). The polymer was collected by filtration, washed with methanol (200 mL), and dried in vacuo at 80 °C for 10 h. Ethylene−propylene copolymerization was performed using a procedure similar to that for ethylene polymerization, except ethylene (100 L/h) and propylene (100 L/h) were used. After the polymerization was terminated, concentrated HCl (2 mL) was added to the resulting mixture, and the mixture was washed with water (250 mL × 3) and concentrated in vacuo. The resultant polymer was dried in vacuo at 130 °C for 10 h. Ethylene−NB copolymerization was performed using a similar procedure, except NB (1 g) was added to the toluene before the ethylene gas feed (50 L/h) was started.

Acknowledgment. We are grateful to the Research Grants Council of the Hong Kong SAR, China [HKU 7095/00P], City University of Hong Kong, and The University of Hong Kong for financial support, and Dr. Duncan F. Wass and Steven C. F. Kui for technical assistance.

Supporting Information Available: CIF files for **3**, **4**, **7**, and Zr(L^1)$_2$; perspective view of Zr(L^1)$_2$; ^{1}H and ^{13}C NMR spectra of selected polyethylene samples. This material is available free of charge via the Internet at http://pubs.acs.org.

OM050864Z

(33) Altomare, A.; Burla, M. C.; Camalli, M.; Cascarano, G.; Giacovazzo, C.; Guagliardi, A.; Moliterni, A. G. G.; Polidori, G.; Spagna, R. *J. Appl. Crystallogr.* **1998**, *32*, 115.